

# Viability of the random pattern dorsal skin flap in mice submitted to photobiomodulation and therapeutic ultrasound

Laís Coan Fontanela<sup>1</sup>, Jaqueline Betta Canever<sup>1</sup>, Aderbal Silva Aguiar Júnior<sup>1,2</sup>, Rafael Inácio Barbosa<sup>1,2</sup>, Marisa de Cássia Registro Fonseca<sup>3</sup>, Heloyse Uliam Kuriki<sup>1,2</sup>, Laís Mara Siqueira das Neves<sup>3</sup>, Alexandre Marcio Marcolino<sup>1,2</sup>

<sup>1</sup>Departamento de Ciências da Saúde, Universidade Federal de Santa Catarina (UFSC) – Araranguá (SC), Brazil

<sup>2</sup>Programa de Pós-Graduação em Ciências da Reabilitação, Universidade Federal de Santa Catarina (UFSC) - Araranguá (SC), Brazil

<sup>3</sup>Programa de Pós-Graduação em Reabilitação e Desempenho Funcional do Departamento de Ciências da Saúde, Faculdade de Medicina de Ribeirão Preto, Universidade de São Paulo (USP) - Ribeirão Preto (SP), Brazil

## ABSTRACT

**Introduction:** The skin flap is a surgical technique widely used in clinical practice and generally presents postoperative complications. Therefore, elucidating interventions that assist in tissue conservation is essential. Photobiomodulation (PBM) and therapeutic ultrasound (TUS) are non-invasive alternatives for assisting tissue repair, however, there is no consensus on the parameters used. **Objective:** To describe the effectiveness of the different parameters of PBM and TUS in the viability of the dorsal random pattern skin flap in mice. **Methods:** Fifty-five *Swiss* mice were used, distributed in eleven groups. The animals were submitted to surgical technique including revascularization of the area limited through a plastic barrier (polyester/polyethylene) with the same dimension as the flap. PBM or TUS was applied for five consecutive days. Photographic and thermographic recordings were performed with Cyber-Shot DSC-P72 and FlirC2 cameras and analyzed using the ImageJ<sup>®</sup> and FLIR Tools software, respectively. In the statistical analysis, the data were submitted to the GraphPad Prism<sup>®</sup> 8.0 software. Analysis of variance (ANOVA Two-way) and Tukey's post-test was performed, considering 5% significance level. **Results:** Groups 5 (PBM 830 nm; 10 J/cm<sup>2</sup>) and 6 (TUS 3 MHz; 0.4 W/cm<sup>2</sup>) showed percentages of viable tissue significantly higher on the third and fifth day of the experiment, when compared to the other groups. The temperature decreased significantly in group 1 when compared to the others in the postoperative period. **Conclusion:** The continuous TUS at 3 MHz and PBM 830 nm were more effective in improving the viability of the dorsal random pattern skin flap in mice.

**Keywords:** low-level light therapy; laser therapy; ultrasound therapy; dermatology; surgery, plastic.

How to cite this article: Fontanela et al. Viability of the random pattern dorsal skin flap in mice submitted to photobiomodulation and therapeutic ultrasound. ABCS Health Sci. 2022;47:e022227 <https://doi.org/10.7322/abcshs.2021013.2122>

Received: Jan 30, 2021  
Revised: Apr 20, 2021  
Approved: May 19, 2021

Corresponding author: Alexandre Marcio Marcolino - Universidade Federal de Santa Catarina, Departamento de Ciências da Saúde - Campus Jardim das Avenidas, Rodovia Governador Jorge Lacerda, 3201 - CEP: 88906-072 – Araranguá (SC), Brazil - E-mail: alexandre.marcolino@ufsc.br

**Declaration of interests:** nothing to declare



This is an open access article distributed under the terms of the Creative Commons Attribution License  
© 2022 The authors

## INTRODUCTION

The skin flap is a surgical technique widely used in plastic surgery for correction or reconstruction, which provides functional and aesthetic improvement of traumatic or congenital defects<sup>1,2</sup>.

The random skin flap corresponds to a portion of tissue from a donor anatomical area that is repositioned in a recipient area, linked using a base, through which the circulation that supplies it passes<sup>3</sup>.

The main cause of failure of the technique is believed to be vasospasm, which acutely interrupts blood flow in the microvasculature and promotes an ischemia-reperfusion injury<sup>4,5</sup>. Once the local blood flow is sufficient, especially in the distal part of the flap, necrosis is no longer a problem<sup>6</sup>.

Thus, studies have been conducted aiming to increase the local blood supply with non-invasive resources, such as Photobiomodulation (PBM)<sup>7,8</sup>. The effects of PBM in the biological system depend on the amount of energy absorbed and the rate of energy deposition<sup>9</sup> so that the wavelength used determines the dispersion and absorption of light<sup>9,10</sup>.

PBM presents several benefits in tissue repair, such as reduction of the inflammatory process<sup>11</sup>, stimulation of fibroblast proliferation, modulation of inflammatory response<sup>12</sup>, modulation of the inflammatory response, increased collagen deposition, and promotion of neoangiogenesis<sup>13</sup>.

In the proliferative phase of tissue repair, the therapeutic ultrasound (TUS) is a resource that also presents positive effects<sup>14</sup>. It highlights early neovascularization<sup>15</sup>, accelerated cellular metabolism<sup>16</sup>, extensibility, and collagen deposition<sup>16</sup>, as factors that may increase tissue survival rates<sup>15,17</sup>.

Because of its thermal and non-thermal effects, TUS has been widely used in soft tissue injuries<sup>15</sup>. By delimiting the parameters of the TUS mechanical waves, it is possible to target the effects on superficial or deep tissue, without causing damage to the outermost part of the skin<sup>18</sup>.

The choice of TUS parameters in the present study was based on previous literature, which showed positive effects on wound healing in rats<sup>14,16</sup>. The PBM parameters were based on previous studies<sup>7-9,12</sup>, which used wavelengths of 660 and 830 nanometers.

However, despite the wide use of these resources in clinical practice, there is little concise evidence about the parameters that should be used<sup>19</sup>. Thus, this study aims to describe the effectiveness of different parameters of PBM and TUS on the viability of the dorsal random skin flap in mice.

## METHODS

The study was carried out at the Animal Facility of the Universidade Federal de Santa Catarina at the Araranguá Campus - SC, with approval from the Ethics Committee on Animal Use of the Universidade Federal de Santa Catarina (CEUA/UFSC) under

number 4017201117. The manuscript was described according to the ARRIVE guidelines.

Sample size analysis was performed, totaling fifty-five animals. The calculation was based on the outcome variable and calculated using G\*Power software, version 3.1, for F-tests, ANOVA with repeated measures, intergroup interaction, F effect size 0.3, significance level  $\alpha$  0.05, power  $(1-\beta)$  0.80, for eleven groups with 3 repeated measures.

We used 55 adult male Swiss mice weighing between 40 and 65 grams. The animals were housed in isolated boxes, each containing five animals, with water and feed available during the entire period of the experiment. The animals were kept under a 12-hour light/dark cycle, with controlled temperature ( $22\pm 2$  °C) and humidity (60-80%).

The treatment was applied for five consecutive days, in which all animals were subjected to the same stress, with the handgrip technique. The animals did not present any kind of diseases before the intervention. On the last day of the protocol, the animals were euthanized with a high dose of anesthesia. The study remained unchanged and there was no sample loss.

## Surgical procedure

Sedation consisted of the intraperitoneal administration of ketamine hydrochloride (Agener União<sup>®</sup>) - 100 mg/Kg associated with xylazine hydrochloride (Dopaser<sup>®</sup>) - 10 mg/Kg, followed by trichotomy by manual traction.

The animals were positioned in ventral decubitus, with their legs extended and their backs free on the surgical table. A 3.0 x 1.5 cm marking was made, totaling an area of 4.5 cm<sup>2</sup>. The upper base of the flap was delimited by the lower angles of the scapulae, so that the base remained intact, allowing the passage of oxygen and nutrients to the flap.

The incision was made caudally, with depth reaching the deep retinaculum of the skin. After the cut, the flap was folded in the cranial direction for the positioning of a plastic barrier (polyester/polyethylene) with the same dimensions as the flap, on the muscle fascia, to limit vascularization only through the base of the flap. The tissue was then repositioned in its origin and sutured with 4.0 monofilament nylon thread.

## Experimental Groups

The animals were randomized into eleven experimental groups, aiming at a comprehensive comparison of the resources used, with different parameters. In group 1 (sham) the animals were submitted to the surgical procedure, being handled under the same stress as the other groups; however, the treatment was performed with the device turned off, aiming only at the placebo effect. The other groups received treatment according to the parameters presented in Tables 1 and 2.

The form of application of the PBM was the same for all experimental groups, punctually with contact below the inferior

**Table 1:** Photobiomodulation parameters used in the treatment of groups 2 to 5

| Group                               | 2     | 3     | 4     | 5     |
|-------------------------------------|-------|-------|-------|-------|
| Wavelength (nm)                     | 660   | 830   | 660   | 830   |
| Power (mW)                          | 30    | 30    | 30    | 30    |
| Output beam (cm <sup>2</sup> )      | 0.6   | 0.11  | 0.6   | 0.11  |
| Power density (mW/cm <sup>2</sup> ) | 16.66 | 19.44 | 16.66 | 19.44 |
| Dose (J/cm <sup>2</sup> )           | 5     | 5     | 10    | 10    |
| Time (s)                            | 10    | 20    | 20    | 40    |
| Energy per point (J)                | 0.3   | 0.6   | 0.6   | 1.2   |

Nm: nanometers; mW: megawatts; cm<sup>2</sup>: square centimeters; s: seconds; J/cm<sup>2</sup>: Joules per square centimeter; J: joules.

**Table 2:** Parameters of therapeutic ultrasound used in the treatment of groups 6 to 11.

| Group                                 | 6          | 7        | 8          | 9        | 10         | 11         |
|---------------------------------------|------------|----------|------------|----------|------------|------------|
| Type of treatment                     | Continuous | Pulsed   | Continuous | Pulsed   | Pulsed     | Pulsed     |
| Type of treatment                     | Circular   | Circular | Circular   | Circular | Stationary | Stationary |
| Frequency (MHz)                       | 3          | 3        | 1          | 1        | 1          | 3          |
| Duty cycle (%)                        | 100        | 20       | 100        | 20       | 20         | 20         |
| Pulse repetition frequency (Hz)       | -          | 100      | -          | 100      | 100        | 100        |
| Intensity - STPA (W/cm <sup>2</sup> ) | 0.4        | 2        | 0.4        | 2        | 0.4        | 0.4        |
| SATA (W/cm <sup>2</sup> )             | -          | 0,4      | -          | 0.4      | 0.08       | 0.08       |
| BNR                                   | 8:1        | 8:1      | 8:1        | 8:1      | 8:1        | 8:1        |

MHz: megahertz; Hz: hertz; W/cm<sup>2</sup>: watts per square centimeter; SATA - spatial average temporal average.

angles of the scapulae, with the pen positioned at 90 degrees. The application of the TUS was performed through circular movements in all groups except 10 and 11, which received the application in a stationary manner over the region during the period of energy emission.

### Photobiomodulation therapy

We used the aluminum, gallium, indium, and phosphorus (AlGaInP) diode laser, which emits a wavelength of 660 nm, and the gallium aluminum arsenide diode laser (AsGaAl) with a wavelength of 830 nm, with a continuous beam, from Ibramed<sup>®</sup> Equipamentos Médicos, São Paulo, Brazil. The parameters used are shown in Table 1.

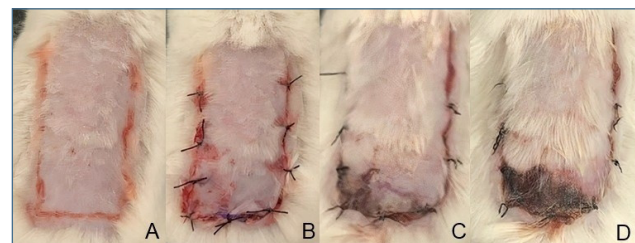
### Therapeutic ultrasound

Table 2 shows the parameters used in the SONOPULSE device (1 and 3 MHz, Ibramed<sup>®</sup>, São Paulo, Brazil). An effective radiation area (ERA) of 1 cm was used<sup>2</sup>, and the TUS application time was 3 minutes for all groups.

### Analysis Procedure

During the experiment, four evaluations of the macroscopic viability area were performed, preoperatively (Figure 1A), immediately postoperative (PO) (Figure 1B), on the third day (Figure 1C), and fifth day (Figure 1D).

The evaluations were performed through photographic records using a digital camera model "Cyber-Shot DSC-P72" (Sony<sup>®</sup>, United States of America), 5.1 megapixels, zoom 3.2. Subsequently, the images were analyzed using ImageJ<sup>®</sup> software.



**Figure 1:** Representation of the area of the dorsal random skin flap on the different days of the experiment. A: Preoperative; B: Postoperative; C: Third day; D: Fifth day.

The temperature was recorded using a FLIR C2 camera (FLIR<sup>®</sup> Systems, Inc.), with a spectral range of 7.5-14  $\mu\text{m}$ , an accuracy of  $\pm 2^\circ\text{C}$  or 2% at  $25^\circ\text{C}$ , and a 320x240 pixels display. The analysis was then performed in FLIR Tools software (FLIR<sup>®</sup>, Systems, Inc.), with the temperature scale maintained from 20 to  $40^\circ\text{C}$ .

All portraits were taken by two independent raters, who were previously trained by an experienced rater. The images were taken in a standardized manner, with distance determined by a twenty-centimeter-high stand.

Throughout the experiment, 440 photographic records were made. The data were tabulated in Microsoft Excel 2019 and checked for differences between raters.

### Statistical Analysis

For statistical analysis, the data were submitted to GraphPad Prism software<sup>®</sup> 8.0 (San Diego, CA, USA) to verify the existence of statistically significant differences between the treatments and parameters used. To analyze data normality the Shapiro-Wilk test

was used, which verified the normal distribution of the sample. For the comparative analysis of the data obtained, the Two-Way ANOVA test was used, followed by Tukey's post-test. All analyses were performed with a 5% significance level.

## RESULTS

In the macroscopic analysis of viability, in the immediate post-operative period, all animals presented 100% of the viable area. The results shown in Figure 2 showed significant differences on the third day between group 10 when compared with G3, G8, G9; group 6 when compared with G1, G2, G3, G8, G9; and group 5 when compared with G1, G2, G3, G8, G9.

On the fifth day of the experiment, the statistically significant differences were between group 10 compared to G1; group 6 compared to G1, G3, G8, G9, and G11; and group 5 compared to G3, G8, and G9, as shown in Figure 2.

Among the groups submitted to PBM treatment, the best result was presented by G5, which was irradiated with PBM with a wavelength of 830 nm and fluence of 10 J/cm<sup>2</sup>, showing approximately 85% viable tissue on the third day and 75% on the fifth day of the study.

Regarding the groups undergoing treatment with TUS, the one that showed the best result was G6, submitted to the frequency of 3 MHz, continuous mode, and intensity of 0.4 W/cm<sup>2</sup>, showing a viable area of 84% on the third day and 86% on the fifth day. Followed by group 10, which performed the treatment with the frequency of 1 MHz, pulsed mode and intensity of 0.4 W/cm<sup>2</sup>, and stationary application mode, expressing 78% and 66% of the viable area on the third and fifth day, respectively.

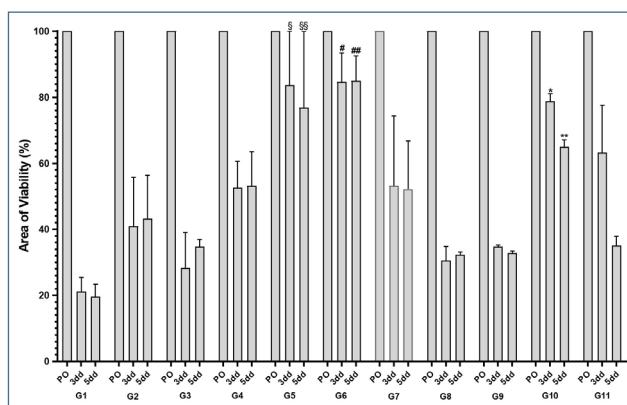


**Figure 2:** Graph of the mean and standard deviation of viable area. Y-axis: viability area (%); x-axis: experimental groups subdivided according to the collections. PO: postoperative; 3dd: third day; 5dd: the fifth day of the experiment. § p<0.05 between G5 and G1, G2, G3, G8, and G9; # p<0.05 between G6 and G1, G2, G3, G8, and G9; \* p<0.05 between G10 and G3, G8 and G9 on the third day of evaluation. §§ p<0.05 between G5 and G3, G8 and G9; ## p<0.05 between G6 and G1, G3, G8, G9, and G11; \*\* p<0.05 between G10 and G1.

All necrotic areas were on the distal part of the skin flaps. None of the groups presented 100% viability, nor 100% necrosis at the end of the study.

Regarding the animals' skin temperature, there was a significant difference only in the PO between G1 when compared to G6, G7, G9, G10, and G11, as shown in Figure 3. The other evaluations showed no significant differences.

## DISCUSSION

The findings show that the group subjected to PBM with a wavelength of 830 nm and fluence of 10 J/cm<sup>2</sup>, showed a larger viable area on the third day (85%). In contrast, the group that showed the highest viability on the fifth day (86%), was the group subjected to TUS, with a frequency of 3MHz, continuous mode, and intensity of 0.4 W/cm<sup>2</sup>.

In this sense, PBM proved to be effective when applied in the short term, corroborating the study of Pouremadi et al<sup>19</sup>, which concluded that PBM was significant in wound healing on the third postoperative day. These results are related to the stimulation of fibroblasts, keratinocytes, and the release of growth factors provided by PBM.

Furthermore, PBM helps in angiogenesis, reducing the percentage of tissue necrosis and consequently increasing the viable area<sup>6-8,20-24</sup>. The parameters used in G5 coincide with the literature, which indicates the wavelength of 830 nm is more promising in neoangiogenesis and tissue healing<sup>23</sup> when compared to 630 nm.

Other studies that also applied PBM with a wavelength of 830nm, showed similar results regarding the increase of viable area<sup>22</sup> and reduction of necrotic areas of the skin flap<sup>7</sup>. The effects of the 830nm wavelength may be related to its ability to penetrate deeply into the tissues<sup>25</sup>.

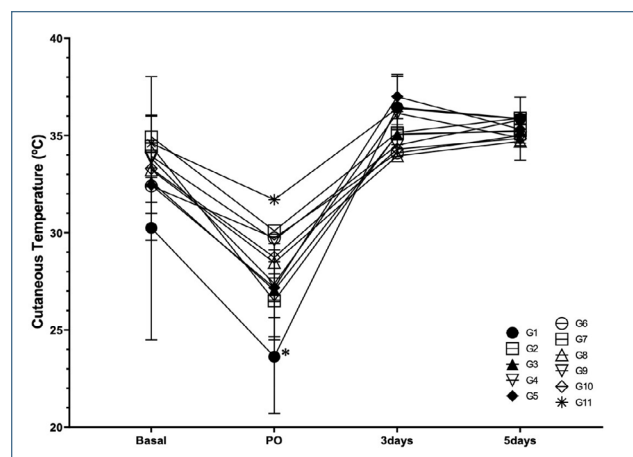


**Figure 3:** Cutaneous temperature. PO: postoperative; 3days: third day and 5days: the fifth day of the experiment. \* p<0.05 between G1 and G6, G7, G9, G10, and G11.

The mechanisms associated with photobioactivation include increased levels of ROS, increased production of adenosine triphosphate (ATP), and release of nitric oxide (NO), as well as increased fibroblast proliferation and consequently, increased collagen and elastin production, deoxyribonucleic acid (DNA) and ribonucleic acid (RNA) synthesis<sup>26</sup>. In addition, the application of PBM at a single point on the flap pedicle area appeared to be superior to multiple irradiations.<sup>27</sup>

When analyzing the viable area on the fifth day of the experiment, TUS obtained more effective results. This finding may be related to morphological changes such as increased epidermal cell proliferation and neoangiogenesis, induced by TUS<sup>28</sup>. Furthermore, microflow generates forces and stresses that can modify the normal configuration of cells and the position of intra- and extracellular particles<sup>29-31</sup>.

The groups treated with TUS that presented the best percentages of viable area (G6 and G10) were submitted to the same intensity of 0.4 W/cm<sup>2</sup>, which may justify the similarity in the results of these groups. Corroborating this finding, the study by Emsen<sup>4</sup> also concluded that TUS may have intensity-related effects to achieve greater skin flap survival.

The study by Yücel et al.<sup>32</sup> analyzed the effect of TUS -assisted preconditioning at a frequency of 3 MHz on ischemic skin flaps, and obtained optimistic results in increased vascular endothelial growth factor (VEGF) and angiogenesis. In addition, the literature evidence that TUS application normalizes microcirculation increases fibroblast synthetic and proliferative activity and initiates macrophage reaction showing early wound closure<sup>4,33</sup>.

The cavitation generated by TUS when applied in a stationary manner may also have influenced tissue viability, considering that

this property increases vascular conductance, being able to reverse ischemia and increase muscle blood flow<sup>34</sup>.

In the evaluation of temperature, a marked reduction is noted after surgical induction in all groups. Anesthesia inhibits several regulatory mechanisms in the body, including those responsible for normothermia<sup>35</sup>. As a consequence, an internal redistribution of heat occurs in an attempt to maintain thermal balance<sup>36</sup>, justifying this sudden drop in temperature.

The control of body temperature provides relevant data to guide the treatment, being a clinical parameter of easy manipulation and understanding<sup>37</sup>. The study by Stadler et al.<sup>38</sup> demonstrated that the application of PBM 830 nm in mice can induce a slight temperature increase on the skin surface, corroborating with the third evaluation of this study, where G5 showed the highest temperature among the groups after the application of PBM 830 nm.

Despite the absence of microscopic analysis, which is a limitation of this study, the effects of TUS and MBP on the viability of the skin tissue were evaluated to provide more knowledge about the use of these resources for tissue repair. On the fifth day, the effects of TUS in G6 and G10 reached better percentages when compared to the groups that received PBM.

Therefore, it is evident that the best results of the groups treated with TUS, the group submitted to the continuous mode and frequency of 3 MHz circular application mode, presented a better result. Among the animals that were treated with PBM, the group with a wavelength of 830 nm showed fewer necrotic regions. When comparing the electrophysical agents and their parameters, we conclude that the TUS is effective in promoting greater viability of the dorsal random skin flap in mice.

## REFERENCES

1. Ferreira LM. Manual de cirurgia plástica. São Paulo: Atheneu, 1995.
2. Enshaei A, Masoudi N. Survey of early complications of primary skin graft and secondary skin graft (delayed) surgery after resection of burn waste in hospitalized burn patients. *Glob J Health Sci.* 2014;6(7):98-102. <https://doi.org/10.5539/gjhs.v6n7p98>
3. Lucas JB. The physiology and biomechanics of skin flaps. *Facial Plast Sur Clin North Am.* 2017;25(3):303-11. <https://doi.org/10.1016/j.fsc.2017.03.003>
4. Emsen IM. The effect of ultrasound on flap survival: an experimental study in rats. *Burns.* 2007;33(3):369-71. <https://doi.org/10.1016/j.burns.2006.08.007>
5. Freitas AD, Padrini Júnior AG, Tavares KE, Lima LAA. Retalhos antebraquiais pediculados para cobertura dos defeitos cutâneos da mão. *Rev Bras Ortop.* 1993;28(4):204-8.
6. Kubota J. Effects of diode laser therapy on blood flow in axial pattern flaps in the rat model. *Lasers Med Sci.* 2002;17(3):146-53. <https://doi.org/10.1007/s101030200024>
7. Neves LMS, Marcolino AM, Prado RP, Thomazini JA. Laser 830nm na viabilidade do retalho cutâneo de ratos submetidos à nicotina. *Acta Ortop Bras.* 2011;19(6):342-5. <https://doi.org/10.1590/S1413-78522011000600004>
8. Neves LMS, Leite GPMF, Marcolino AM, Pinfildi CE, Garcia SB, Araújo JE, et al. Laser Photobiomodulation (830 and 660 Nm) in Mast Cells, VEGF, FGF, and CD34 of the musculocutaneous flap in rats submitted to nicotine. *Lasers Med Sci.* 2017;32(2):335-41. <https://doi.org/10.1007/s10103-016-2118-1>
9. Yadav A, Gupta A. Noninvasive red and near-infrared wavelength-induced photobiomodulation: promoting impaired cutaneous wound healing. *Photodermatol Photoimmunol Photomed.* 2017;33(1):4-13. <https://doi.org/10.1111/phpp.12282>
10. Freitas LF, Hamblin MR. Proposed mechanisms of photobiomodulation or low-level light therapy. *IEEE J Sel Top Quantum Electron.* 2016;22(3):7000417. <https://doi.org/10.1109/JSTQE.2016.2561201>

11. Guirro ECO, Montebelo MIL, Bortot BA, Torres MACB, Polacow MLO. Effect of Laser (670 Nm) on the healing of wounds covered with occlusive dressing: a histologic and biomechanical analysis. *Photomed Laser Surg.* 2010;28(5):629-34. <https://doi.org/10.1089/pho.2008.2387>
12. Fortuna T, Gonzalez AC, Sá MF, Andrade ZA, Reis SRA, Medrado ARAP. Effect of 670 Nm laser photobiomodulation on vascular density and fibroplasia in late stages of tissue repair. *Int Wound J.* 2018;15(2):274-82. <https://doi.org/10.1111/iwj.12861>
13. Melo VA, Anjos DCS, Albuquerque Júnior R, Melo DB, Carvalho FUR. Effect of low level laser on sutured wound healing in rats. *Acta Cir Bras.* 2011;26(2):129-34. <https://doi.org/10.1590/S0102-86502011000200010>
14. Taşkan I, Ozyazgan I, Tercan M, Kardeş HY, Balkanlı S, Saraymen R, et al. A comparative study of the effect of ultrasound and electrostimulation on wound healing in rats. *Plast Reconstr Surg.* 1997;100(4):966-72. <https://doi.org/10.1097/00006534-199709001-00020>
15. Chen YC, Wang PR, Lai TJ, Lu LH, Dai LW, Wang CH. Using therapeutic ultrasound to promote irritated skin recovery after surfactant-induced barrier disruption. *Ultrasonics.* 2019;91:206-12. <https://doi.org/10.1016/j.ultras.2018.08.007>
16. Carrer V, Setti JAP, Veronez DL, Moser AD. Ultra-som terapêutico contínuo no processo de cicatrização na pele de ratos. *Fisioter Mov.* 2015;28(4):751-8. <http://dx.doi.org/10.1590/0103-5150.028.004.AO12>
17. Wakabayashi N, Sakai A, Takada H, Hoshi T, Saco H, Ichinose S, et al. Noncontact phased-array ultrasound facilitates acute wound healing in mice. *Plast Reconstr Surg.* 2020;145(2):348e-59. <https://doi.org/10.1097/PRS.0000000000006481>
18. Matthews MJ, Stretanski MF. *Ultrasound Therapy.* StatPearls, 2020.
19. Pouremadi N, Motaghi A, Safdari R, Zarean P, Rashad A, Zarean P, et al. Clinical outcomes of low-level laser therapy in the management of advanced implant surgery complications: a comparative clinical study. *J Contemp Dent Pract.* 2019;20(1):78-82.
20. Kami T, Yoshimura Y, Nakajima T, Ohshiro T, Fujino T. Effects of low-power diode lasers on flap survival. *Anna Plast Surg.* 1985;14(3):278-83. <https://doi.org/10.1097/00000637-198503000-00013>
21. Pinfildi CE, Liebano RE, Hochman BS, Ferreira LM. Helium-neon laser in viability of random skin flap in rats. *Lasers Surge Med.* 2005;37(1):74-7. <https://doi.org/10.1002/lsm.20190>
22. Prado R, Neves L, Marcolino A, Ribeiro T, Pinfildi C, Ferreira L, et al. Effect of low-level laser therapy on malondialdehyde concentration in random cutaneous flap viability. *Photomed Laser Surg.* 2010;28(3):379-84. <https://doi.org/10.1089/pho.2009.2535>
23. Souza TR, Souza AK, Garcia SB, Neves LMS, Barbosa RI, Guirro RRJ, et al. Photobiomodulation increases viability in full-thickness grafts in rats submitted to nicotine. *Lasers Surg Med.* 2020;52(5):449-55. <https://doi.org/10.1002/lsm.23155>
24. Kubota J. Defocused diode laser therapy (830 Nm) in the treatment of unresponsive skin ulcers: a preliminary trial. *J Cosmet Laser Ther.* 2004;6(2):96-102. <https://doi.org/10.1080/14764170410014983>
25. Calderhead RG, Kim WS, Ohshiro T, Trelles MA, Vasily DB. Adjunctive 830 nm light-emitting diode therapy can improve the results following aesthetic procedures. *Laser Ther.* 2015;24(4):277-89. <https://doi.org/10.5978/islsm.15-OR-17>
26. Kim WS, Calderhead RG. Is light-emitting diode phototherapy (LED-LLLT) really effective?. *Laser Ther.* 2011;20(3):205-15. <https://doi.org/10.5978/islsm.20.205>
27. Hersant B, SidAhmed-Mezi M, Bosc R, Meningaud JP. Current indications of low-level laser therapy in plastic surgery: a review. *Photomed Laser Surg.* 2015;33(5):283-97. <https://doi.org/10.1089/pho.2014.3822>
28. Gonçalves AC, Barbieri CH, Mazzer N, Garcia SB, Thomazini JA. Can Therapeutic Ultrasound Influence the Integration of Skin Grafts?. *Ultrasound Med Biol.* 2007;33(9):1406-12. <https://doi.org/10.1016/j.ultrasmedbio.2007.04.002>
29. Kitchen SS, Partridge CJ. A review of therapeutic ultrasound: I. Background, physiological effects and hazards. *Physiotherapy.* 1990;76:593.
30. Dyson M. Mechanisms Involved in therapeutic ultrasound. *Physiotherapy.* 1987;73(3):116-30.
31. ter Haar G. Therapeutic ultrasound. *Eur J Ultrasound.* 1999;9(1):3-9. [https://doi.org/10.1016/s0929-8266\(99\)00013-0](https://doi.org/10.1016/s0929-8266(99)00013-0)
32. Yücel S, Günay GK, Ünverdi ÖF. Effects of ultrasound-assisted preconditioning on critically ischemic skin flaps: an experimental study. *Ultrasound Med Biol.* 2020;46(3):660-6. <https://doi.org/10.1016/j.ultrasmedbio.2019.12.009>
33. Gostishchev VK, Baichorov EK, Berchenko GN. Effect of low-frequency ultrasound on the course of the wound process. *Vestn Khir Im I I Grek.* 1984;133(10):110-3.
34. Belcik JT, Davidson BP, Xie A, Wu MD, Yadava M, Qi Y, et al. Augmentation of muscle blood flow by ultrasound cavitation is mediated by atp and purinergic signaling. *Circulation.* 2017;135(13):1240-52. <https://doi.org/10.1161/CIRCULATIONAHA.116.024826>
35. Planel E, Richter KE, Nolan CE, Finley JE, Liu L, Wen Y, et al. Anesthesia leads to tau hyperphosphorylation through inhibition of phosphatase activity by hypothermia. *J Neurosci.* 2007;27(12):3090-7. <https://doi.org/10.1523/JNEUROSCI.4854-06.2007>
36. Matsukawa T, Sessler DI, Sessler AM, Schroeder M, Ozaki M, Kurz A, et al. Heat flow and distribution during induction of general anesthesia. *Anesthesiology.* 1995;82(3):662-73. <https://doi.org/10.1097/0000542-199503000-00008>
37. Fiebig K, Jourdan T, Kock MH, Merle R, Thöne-Reineke C. Evaluation of Infrared Thermography for Temperature Measurement in Adult Male NMRI Nude Mice. *J Am Assoc Lab Anim Sci.* 2018;57(6):715-24. <https://doi.org/10.30802/AALAS-JAALAS-17-000137>
38. Stadler I, Lanzafame RJ, Oskoui P, Zhang RY, Coleman J, Whittaker M. Alteration of skin temperature during low-level laser irradiation at 830 Nm in a mouse model. *Photomed Laser Surg.* 2004;22(3):227-31. <https://doi.org/10.1089/1549541041438560>